Accepted for Publication in Journal of the Mechanical Behavior of Biomedical Materials

Surface Modification for Osseointegration of Ti6Al4V ELI using Powder Mixed Sinking EDM

Mohammad Pervez Mughal[1], Muhammad Umar Farooq[1*], Jabir Mumtaz [2], Mozammel Mia[3*], Madiha Shareef[1], Mahnoor Javed[1], Muhammad Jamil[4], Catalin I. Pruncu[3,5]

[1]Department of Industrial and Manufacturing Engineering, University of Engineering and Technology, Lahore mp_mughal@uet.edu.pk (M.P.M); madiha.1996@gmail.com (M.S); mahnoorj298@gmail.com (M.J)

[2]Department of Mechanical Engineering, University of Lahore, Islamabad jabirmumtaz@me.uol.edu.pk (J.M)

[3]Department of Mechanical Engineering, Imperial College London, Exhibition Rd., SW7 2AZ, London, UK c.pruncu@imperial.ac.uk (C.I.P)

[4]College of Mechanical and Electrical Engineering, Nanjing University of Aeronautics and Astronautics, Nanjing, 210016, China engr.jamil@nuaa.edu.cn (M.J)

[5]Design, Manufacturing & Engineering Management, University of Strathclyde, Glasgow G1 1XJ, Scotland, UK

* corresponding author muf@uet.edu.pk, m.mia19@imperial.ac.uk

Abstract

Biomedical implant rejection due to micromotion and inflammation around an implant leads to osteolysis and eventually has an implant failure because of poor osseointegration. To enhance osseointegration, the implant surface modification both at the nano and micro-scale levels is preferred to result in an enhanced interface between the body tissue and implant. The present study focuses on the modification of the surface of Titanium (α+β) ELI medical grade alloy using powder-mixed electric discharge machining (PMEDM). Pulse current, on/off time, and various silicon carbide (SiC) powder concentrations are used as input parameters to comprehend desired surface modifications. Powder concentration is considered as the most important factor to control surface roughness and recast layer depth. A significant decrease in surface fracture density and roughness is observed using a 20g/l concentration of SiC particles. Elemental mapping analysis has confirmed the migration of Si and the generation of promising surface texture and chemistry. Oxides and carbides enriched surface improved the microhardness of the re-solidified layer from 320HV to 727HV. Surface topology reveals

nano-porosity (50-200nm) which enhances osseointegration due to the absorption of proteins especially collagen to the surface.

Keywords Titanium Implants, Ti6Al4V, Osseointegration, EDM, Surface Modification, Silicon Diffusion, Surface chemistry

1. Introduction

Titanium and its alloys have gained popularity in permanent implants (orthopedics and dental) because of their outstanding properties such as high toughness, strength to weight ratio good surface stability in highly oxidizing environments, corrosion resistance, biocompatibility, and low cytotoxicity properties (Freese et al., 2001). Ti6Al4V, ($\alpha+\beta$) alloy is extensively used in the biomedical, aeronautical, automotive industry, chemical plants, power generation, and other industries. For biomedical applications, the success rate is as high as 82.94% over a long term analysis (Simonis et al., 2010). To further this success, Ti6Al4V extra low interstitial (ELI) grade 23, a variant of Ti6Al4V grade 5 is developed having lower levels of C, O, Fe and N; thus, providing higher resistance to corrosion, better fracture toughness and 25% higher ductility than Ti6Al4V grade 5 (Umar Farooq et al., 2020; Watanabe et al., 2015). However, similar to other titanium alloys, machinability of Ti6Al4V ELI grade 23 (T64 ELI) is challenging because of its hardness, large coefficient of friction, wear-resistance and minor thermal conductivity; resulting in difficulty to achieve integrity of surface and accuracy in dimensional parameters using conventional machining processes (Mishra et al., 2019).

Non-conventional machining paradigm like electric discharge machining (EDM) is utilized due to little or no involvement of mechanical forces which eliminates the difficulties of hardness and other mechanical properties which makes the material hard-to-cut (Malhotra et al., 2008). Repetition of melting action and re-solidification of the material surface during the process cause major changes in the metallurgical properties and grain size in the recast layer (Singh et al., 2018). The drawbacks associated with the process are re-solidified layer due to insufficient flushing, higher tool wear rates and lower dimensional accuracy (Dewangan et al., 2015). Recent advancements in the EDM process are the addition of micro and nano-powders, surfactants, utilization of

ultrasonic-assisted electrodes, rotary electrodes, and magnetic stirring technology to name a few. An addition of powder in dielectric enhances the spark density on the surface due to the suspension of the additives (Ying et al., 2017). It mainly improves the material removal rate (MRR), surface roughness (SR), recast layer thickness (RLT), wear and corrosion resistance and micro cracks (Çogun et al., 2006).

The chemical composition of implants and surface topography are important factors for Vitro and Vivo osseointegration (Park et al., 2009). It is observed in recent research that nano-structured titanium can give significant osteointegration as compared to titanium by micro-scale surface modifications. The nano-scale surfaces which have increased surface area, have the ability to absorb proteins, and increase cell adhesion, proliferation, and tissue integration (Cai et al., 2006; Zeng et al., 2019). Various post-processing operations are studied to modify the implant surface. These processes include sol-gel (Miao et al., 2011), sputter processes (Zeng et al., 2019), dip coating (Sollazzo et al., 2008), hot pressing (Hassanin et al., 2017) just to name a few. Despite, the benefits of these processes, some drawbacks are also associated with them like the need for a controlled atmosphere, higher cost, time-consuming and poor adhesion (Subramani et al., 2018). In orthopedics, an implant requires low surface roughness, high mechanical strength, and good biocompatibility to avoid inflammation (Ahmed et al., 2012). Different conventional and non-conventional machining operations are used to manufacture biomedical implants. Due to the challenging needs of surface roughness and topography, dimensional accuracy, and other factors, non-conventional machining processes are preferred. After machining of implant, different post-treatment processes, enhance the capabilities of bioactivity and biocompatibility (Saptaji et al., 2018). Electric discharge machining (EDM) has a preferred use in the machining of the implants due to the generation of bioactive surfaces, open pores, and deposition of minerals which make it compatible with the human body environment. Selection of electrode, workpiece, and machining parameters is required intelligently to achieve the goal (Kumar et al., 2009).

EDM has a better potential for surface modification as compared to other physical and chemical vapor deposition techniques. Though surface modification through EDM research is at initial stages therefore, extensive studies are required for the selection of parameters to produce better biocompatible surfaces (Abu Qudeiri et al., 2018). Holmberg et al., 2019 compared the laser beam machining (LBM), EDM and abrasive water jet cutting (AWJC)

where AWJC and EDM were found most suitable for the machining of Alloy 718. The results represent that EDM produced an uneven recast layer on the surface and the coarser surface as compared to AWJC. Tiwary et al., 2018 evaluated MRR, tool wear ratio (TWR), dimensional accuracy and taper of Ti6Al4V using different dielectrics. The study revealed that MRR increased with an increase in pulse current, while no recast layer was found with Cu powder mixed deionized water. Liang et al., 2018 studied the generation of a modified surface where EDM produced an oxygen plasma etching and reduced surface defects which ultimately increased the fatigue strength of Ti6Al4V. Kolli and Kumar, 2015 studied the differences between the surfactant and graphite powder mixed dielectric on MRR, SR and recast layer. It was found that surface roughness (SR) is directly related to pulse current and inverse in proportion to surfactant and powder concentration. RLT initially increased (4-6g/l) and then decreased (6-8g/l) which was found directly proportional to powder concentration and pulse current. Hadad et al., 2018 evaluated the surface roughness of the workpiece and electrode and found that the surface roughness of the workpiece was slightly depended on the initial surface roughness of an electrode. Furthermore, MRR decreased with, initially coarser electrode. Jahan and Alavi, 2019 ensured the conversion of material from an electrode to the workpiece and due to this conversion of carbon from the dielectric, microhardness was slightly increased. Singh and Singh, 2015 evaluated the powder concentration which resulted in an initial decrease in surface roughness and then an increase was observed on Al6063 Aluminum Alloy. An identical study was reported with boron carbide powder (Kolli and Kumar, 2014). Alavi and Jahan, 2017 studied the effect of electrode coating (uncoated tungsten carbide, TN coated tungsten carbide), servo voltage, capacitance and rotational speed on MRR, TWR, microhardness and crater size on Ti6Al4V. The study revealed that voltage was a significant factor for machining time and crater while capacitance was found significant on microhardness and TWR. Kumar et al., 2018 utilized multi-objective optimization of parameters for machining of Monel 400 alloy using copper–titanium diboride powder metallurgy electrode and found pulse current to affect MRR and TWR. Sahu et al., 2018 examined Inconel 718 superalloys under SiC mixed EDM which resulted in a lower crack density of the machined surface, better surface morphology due to reduced surface irregularities and significant grain refinement. However, the powder concentration was not evaluated in the study and the researcher proposed an urgent need of the study based on different concentrations of powder

on surface asperities. Somashekhar et al., 2010 optimized MRR by artificial neural networks and genetic algorithms. Suresh et al., 2016 evaluated copper, brass and graphite electrodes on Ti6Al4V grade 5 for surface roughness and dimensional accuracy. A graphite electrode resulted in minimum SR as compared to other electrodes.

It has been observed from the literature that previous research has been focused on controllable parameters to improve MRR, TWR, SR. The role of powder concentration on the surface modification of Ti64 ELI (grade 23) has not been comprehensively studied, however, this has proved advantages as evident from literature. Furthermore, no substantial work has been done in the evaluation of pulse current and pulse on/off time on the surface characteristics of Ti64 ELI (grade 23) which is a potential biomedical material having a wide range of applications. Öpöz et al., 2018 evaluated surface roughness, deposited particles, surface topography and microhardness of Ti6Al4V in SiC mixed EDM. The study evaluated pulse current, pulse on time and concentration of powder using the Aluminum 6081 T6 electrode. The study shows that powder concentration was the most influential factor in responses and the RLT decreased by increasing the concentration of powder while layer hardness increased due to migrated material. Prakash et al., 2017 explored the porosity produced by powder mixed-electric discharge machining (PMEDM). The study resulted in the addition of Si powder decreased surface roughness and increased surface favorable characteristics. Shabgard and Khosrozadeh, 2017 revealed that the addition of carbon nanotubes decreased surface cracks. The literature revealed that powder mixed EDM has a broader scope in surface modification of different materials as compared to other machining processes (Umar Farooq et al., 2020). Ti64 ELI (grade 23) is a specially developed alloy for biomedical implants that need surface modification to enhance the biocompatibility in Vitro and Vivo environments. The strength of the work has been to delve into surface features produced from the process (EDM) which simultaneously serves as machining as well as surface modification method. Moreover, powder mixed EDM surface modification of Ti64 ELI (grade 23) is explored to evaluate the impact of powder concentration, pulse current as well as a pulse on:off time on surface integrity for specialized applications in the biomedical industry. Furthermore, the work focuses on the quality enhancement of said material's surface to improve mechanical behavior as well as bioactivity.

2. Methodology

In the present study, a 2.5 mm thick plate of Ti6Al4V ELI (grade 23) is employed as a workpiece with a copper electrode (15mm DIA) and SiC mixed dielectric. The elemental composition of Ti64 ELI was confirmed using inductively coupled optical (ICP) emission spectrum analysis and is shown in Table 1. Radial ICP was used because of its better refractory Si, Ti etc. The material is loaded in the setup and spectrum of radiations specifically electromagnetic are emitted making an atom's high energy state to low energy state. The unique emission spectrum is used to identify elements from the unknown composition. Two samples were tested to verify the composition, provided by the manufacturer. The mechanical characteristics are presented in Table 2 (Niinomi, 1998). The properties of the electrode used and SiC powder are presented in Tables 3 and 4 respectively. EDM die sinker (Rj-230) was used for experimentation; to ensure proper suspension of SiC particles and effective flushing, the dielectric bath was modified with additional pumps. The overall process schematic is presented in the illustration, Fig 1.

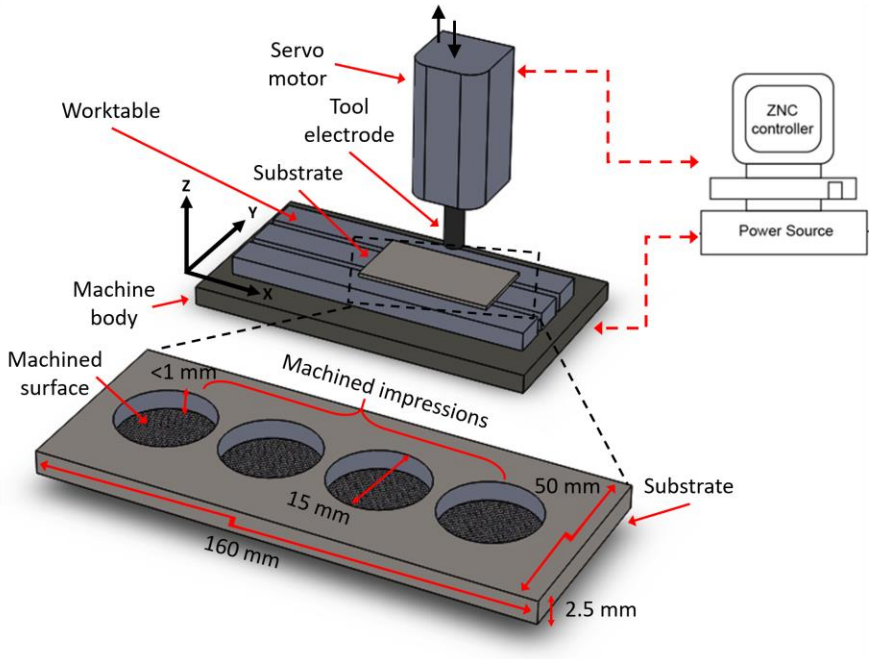

Figure 1. Schematic diagram of EDM machine.

During the trial experiments, the effects of machining using negative electrode polarity were found better against positive electrode polarity, therefore, negative electrode polarity is applied in the present work. Because the negative polarity mainly focuses on machining rather solely performing deposition. Powder concentration (C_p), pulse current (Ip) and pulse on:off times were selected as input parameters as reported in Table 5, and constant parameters are given in Table 6. A full-factorial design was used for experiments containing 36 experiments in which 9 experiments were carried out without adding powder as shown in Table 7. Each experiment was repeated three times to nullify the effect of variance caused by external factors. The significance analysis (mentioned in Table 8) to investigate the parametric effect was also carried out to select the baseline for improvement. The SR was measured using the surface texture meter. The values of surface roughness (Ra) presented are an average of five values from different regions of the finished surface. The detailed topological assessment was done on EDS which was equipped with Quanta 450 Field Emission Gun (FEG) and SEM which is known as Scanning Electron Microscopy (SEM). The analysis and re-solidified layer have examined on INSPECT S50 SEM. The crater sizes were analyzed on measuring microscope OLYMPUS STM6-LM.

Machined samples which are sectioned by CNC Wire EDM to investigate subsurface properties. Moreover, all the sectioned samples were heat molded and sanded using 200-2000 size of mesh, sandpapers and were polished with 0.5-1μm diamond paste. The Vickers hardness values were measured using the Vickers Hardness Tester, HMV G21. The results of microhardness are explained in the results and discussion section. For the measurement of the recast layer, machined samples were cross-sectioned and polished. The polished face is further explored to investigate surface layer properties. The thickness of various regions on the face known as the recast layer in heat-affected zone (HAZ) was measured using ImageJ software. ImageJ software is an image processing application in which measurement facilities are available. At the start, the pixel to measurement scale ratio is adjusted. After that desired regions are measured using reference point and the destination point. Twenty regions on each sample were selected and measured by taking reference measuring scale provided by microscope. Table 9 shows the average of recast layer thickness measured. Minitab 19 software was used for the construction of the main effect plots. The total number of samples for surface quality examination was 36 (N= 36). Surface roughness and recast layer thickness on powder mixed setup was investigated (n= 27).

Moreover, additional 9 experiments were carried out to explicitly discuss the surface quality improvement (n= 9) at zero powder concentration. To explore surface topography, layer features obtained on all powder concentrations and pulse current levels were categorized (n= 12). For the porosity and hardness, three different powder concentrations (n= 3) were investigated for surface characteristics improvement and to plot the heat-affected zone, respectively. The elemental analysis is carried out on the optimized set of parameters obtained from desirability approach (n= 1). Statistical analyses such as analysis of variance to determine the influence of input variables on the responses are carried out. It glorifies the most impactful variables which potentially control the output and changing these variables majorly affect yield. Moreover, analysis of means also called main effect plot describes the trends of the variables in which the effect is varied. It has been carried out to understand the influence of process variables on surface properties to better optimize the key features.

3. Results and Discussion

As discussed earlier, surface characteristics i.e., surface roughness, surface chemistry, recast layer thickness and nano-topography helps to find the biocompatibility of substrate and optimization for spreading, proliferation and adhesion of cells. Sub-micron SR with nanoscale topography enhances Vitro and Vivo osseointegration.

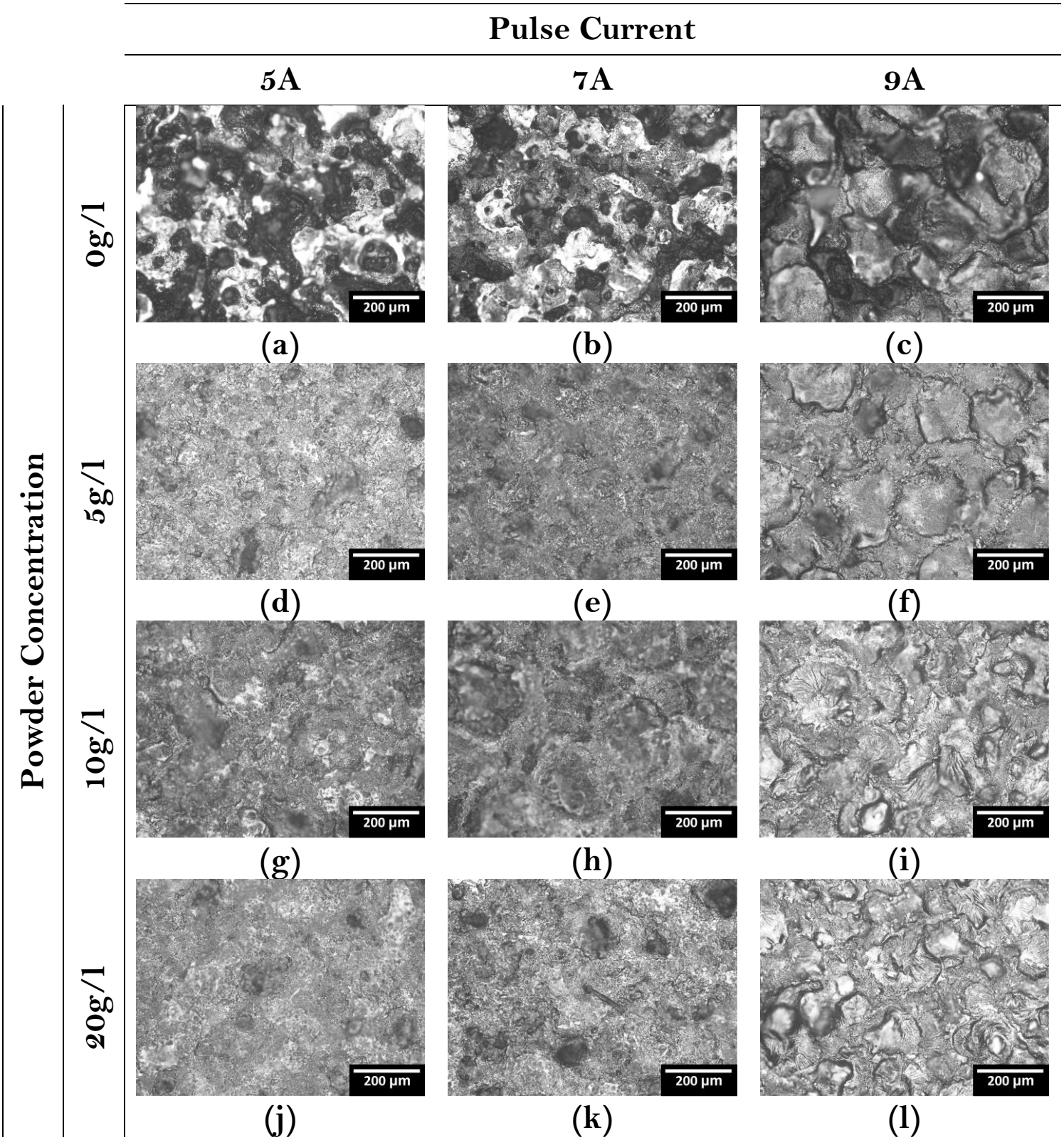

Figure 2. Surface topography: images of samples at 50 µSec pulse on time and 200x magnification

3.1 Surface Topography and Morphology:

Fig 2 shows the surface topographies of the machined surfaces for various currents and powder concentrations.

As the pulse current gradually increases, the evidence of redeposited particles, molten metal and the depth and

size of craters increase. Fig 2 (a-c), show the surface morphology on the EDM surface with 0 g/l concentration. The experimental runs on 0 g/l powder concentration are shown in Table 7 and the pulse current has been significant parameter in controlling surface properties as evident from Table 8. At 5A pulse current and 50µSec pulse-on time, large areas of discharge craters, edges of redeposited molten metal, sharp-edged marks and surface cracks were formed. Clearly visible subtle surface asperities are formed by EDM without the addition of powder which causes pebbling like uneven surface. While with the increment in pulse current from 5A to 9A; the density and size of craters increase. Poor surface quality is experienced at higher pulse current probably due to high discharge energy coupled with poor discharge density. Which leads to non-uniform melting and re-solidification thus, making discharge craters and ridges on the machined surface. The re-solidified metal forms oxides and carbides, allowing spherical coarse grain growth and causing a poor surface texture and characteristics. Fig 2 (d-f) show the micrographs of EDM with 5g/l powder concentration mixed in a dielectric with 50µSec pulse on-time and the three pulse currents. The surface topography at low pulse current (5A) yields finer and small craters forming an even surface while, at high discharge current i.e., 9A, surface topology is still highly non-uniform. However, due to the addition of powder, the size of pits/craters reduced from (150-200µm) to (50-120µm) with a reduced crack density. Powder concentration was enhanced to 10 g/l and later to 20 g/l, which resulted in reduced ridges and smaller size of discharge craters (10-20µm) as shown in Fig 2 (j-i). Using a high concentration of SiC 20 g/l more sparks locations (density) and frequency results in a good distribution of energy which assists in decreasing the energy per spark that resulted in small craters. Further, due to highly distributed spark, metal erosion results in small debris, which was easy to flush, resulting in a better surface finish and reduced surface defects. Surface roughness results are presented in tables 7 and 8 showing the variations between 5.5 µm and 8.5 µm. Analysis of variance using ANOVA yields 67.7 % contribution of pulse current (A) in controlling the surface roughness with a p-value of 0.031 which is the only significant factor.

Results of the twenty-seven experiments conducted with SiC powder mixed dielectric are presented in Table 9. ANOVA analysis for determination of the significant controlling factors reveals that the most significant factor is powder concentration which controls the recast layer thickness with a 70.55 % contribution, followed by interaction of powder concentration and pulse current with a contribution of 15.88% as shown in table 10. Due

to the successive discharges application, an overlapped craters surface can be witnessed in Fig 3. The crater rims and spherical structures are identified on the surface due to molten material flow and redeposition. These features tend to solidify due to direct heat transfer in dielectric and conduction to the base material. As it has been illustrated from Fig 4, the addition of SiC powder in dielectric alters the failure conditions during discharging which results in improved surface topography under specific control parameters. Initially, Fig 3 (a) in the case of 50μSec pulse-on time, 5A pulse current and 5 g/l particle concentration in the dielectric comparatively fine surface is obtained as compared to EDM without powder.

Larger crater channels are still witnessed due to primary discharges in Fig 3 (a, b) but the major discharge channel activity seems to be blocked as by increasing SiC powder concentration in Fig 3 (c, d). While channel activity dissipated, and almost crack-free surface obtained with 20g/l powder concentration as shown in Fig 3 (e, f). Microcracks redeposited debris and SiC particles from dielectric have been identified throughout the process surface texture. It can be concluded that by increasing powder concentration; micro surface defects reduced comparatively in high density as compared to lower concentration and without powder EDM.

The addition of SiC in dielectric helps growth in the gap for discharge and the failure of the dielectric medium strength which is also decreased. Due to this fact, early discharges occur among the suspended particles. Improved discharge dispersal and enlarged gaps facilitate debris to flush away efficiently. The process becomes steadier where necessary flushing of debris is expected. It is mainly depended on abrasive particle concentration, size, electrical and thermal conductivity, melting point, and specific heat, etc., which play a vital role during machining. The addition of SiC in dielectric ensures improved electrical and thermal conductivity. The contribution of aforesaid parameters promotes solidification of molten metal, decomposition of dielectric and particle migration from powder to a surface (Umar Farooq et al., 2020).

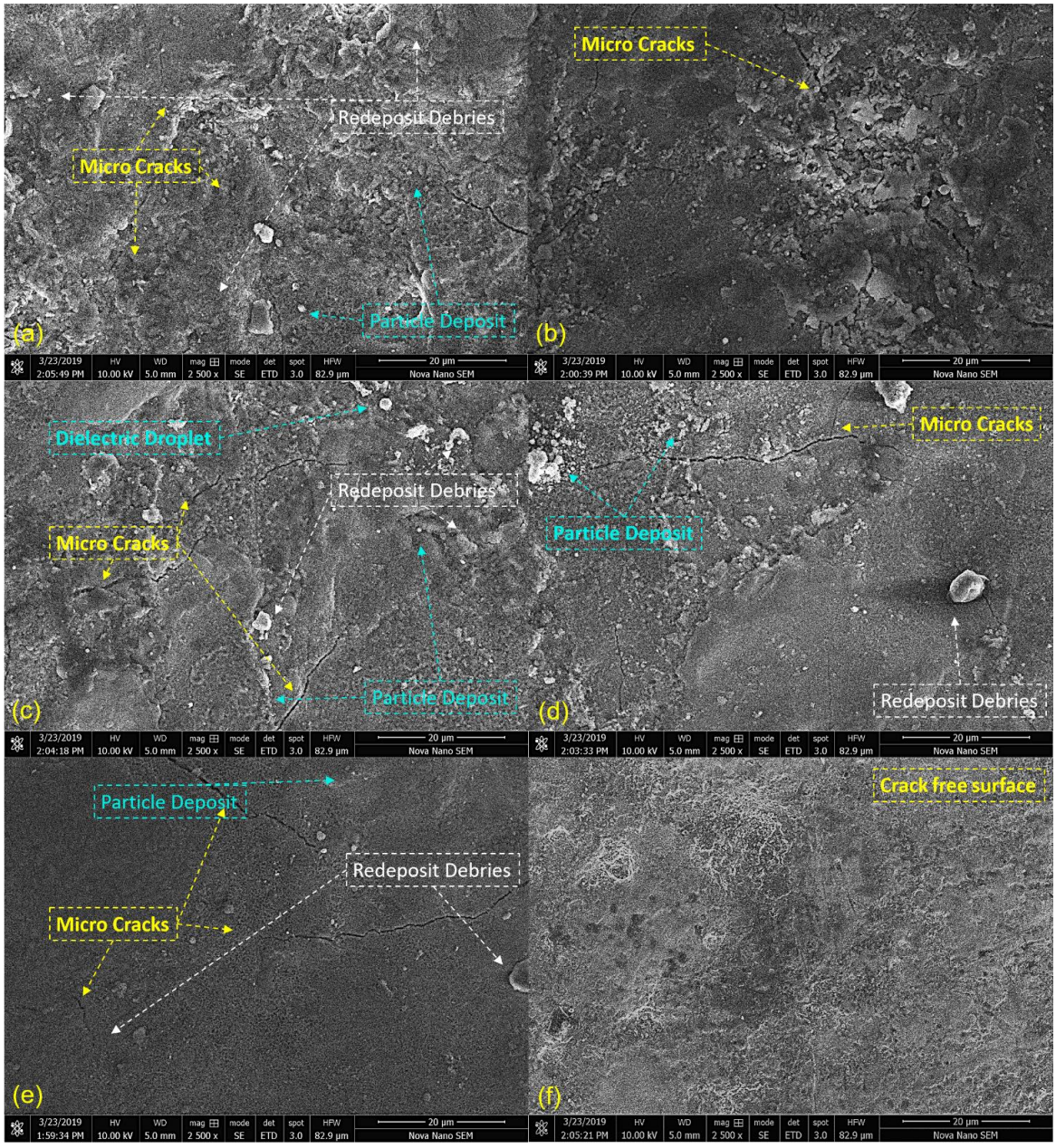

Figure 3. SEM micro-graphs of Ti6Al4V ELI (grade 23) modified surface at IP 5A, TON 50µSec and SiC powder concentration CP (a,b) 5g/l, (c,d) 10g/l, (e,f) 20g/l at 2500x magnification.

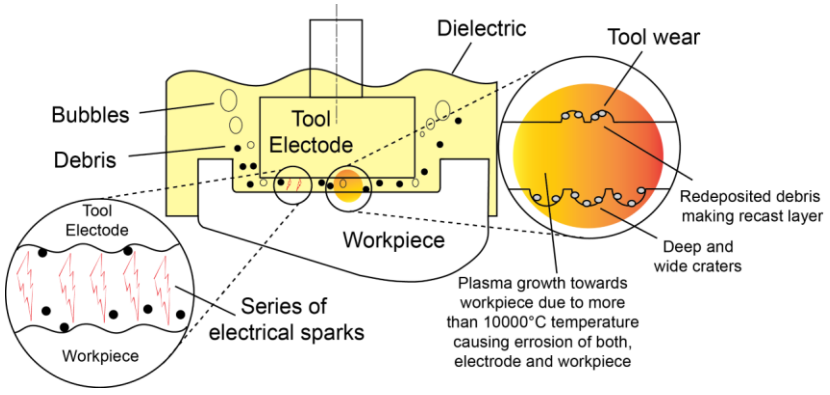

Figure 4. Schematic of material removal for EDM detailed process which gives high surface roughness.

3.2 Modified Layer Analysis:

The present study evaluates the thickness of machined samples recast layer in SiC mixed dielectric. The recast layer was observed in almost all machined samples. This is because of the localized agglomeration of the excess of powder in the gap which restricts the molten metal debris from flush away properly. Therefore, molten metal gets solidified on the surface generating the recast layer. In very few samples unified and the thinner recast layer was observed.

RLT has a direct relation to the concentration of suspended powder in the dielectric, pulse current and pulse on-off time. Fig 5 shows micrographs of cross-sectioned machined samples RLT at 5g/l, 10g/l, and 20g/l powder concentration. It is observed that at 5g/l concentration (~6-10µm thick) RLT was obtained as shown in Fig 5 (a). Powder concentration remarkably affects RLT as it increased by increasing powder concentration. As concentration further increases to 10g/l, RLT increased (~15-40µm thick) and recast layer thickness was measured about (~20-50µm thick) on 20g/l under the same working conditions as shown in Fig 5 (b, c).

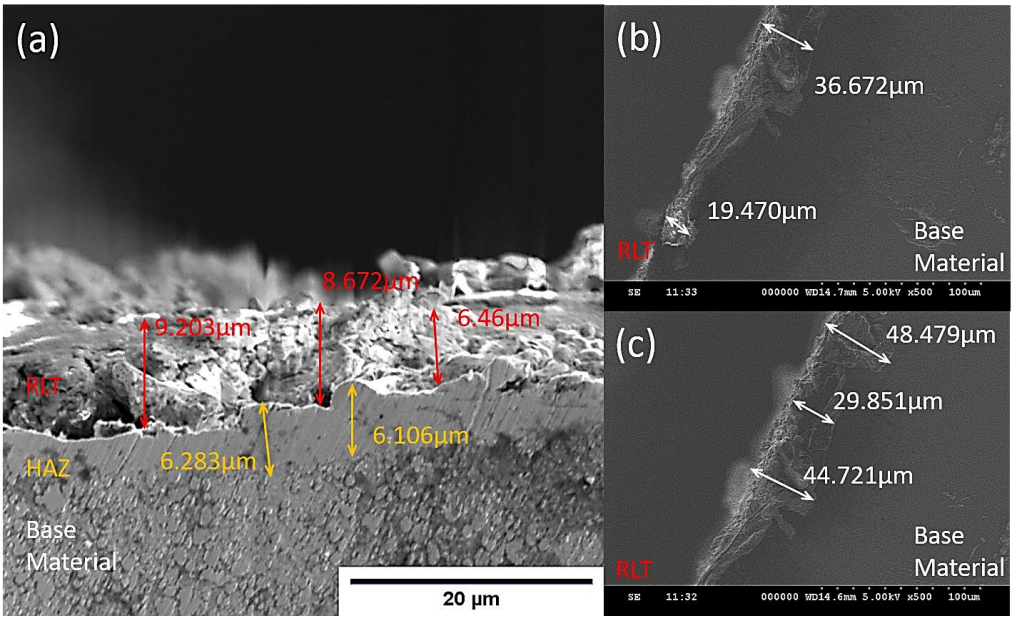

Figure 5. Cross-section SEM micrographs of recast layer thickness of SiC mixed EDMed samples with powder concentration (a) 5g/l (b) 10g/l (c) 20g/l at 500x and 1500x magnification

RLT is majorly depended on C_P, I_P, and T_{ON}. At higher concentrations of powder, powder particles get entrapped with debris between the interspace and cannot flush out. Therefore, they are shifted to the surface of the workpiece and get solidified there, making ridges of redeposited material in the form of a recast layer

ultimately increasing its thickness which improves surface hardness. Suspending SiC powder into the dielectric fluid produces a huge gap compared to EDM which helps the flushing process and makes the process more stable.

3.3 Surface Porosity:

The nano-porous surface and nano feature surface was fabricated on the machined surface. Open porosity is generated on a modified surface which favorably promotes osseointegration. Various studies have been found EDM based surface modification for the enhancement of Osseo-conductivity of titanium and its alloys. It has been verified that the surface treated by EDM provides an extended opportunity for osteoblast cell attachment (Chen et al., 2008). Nano-porous surface generated on Ti implant adapted by EDM has found a considerable impact on adhesion and proliferation of human osteoblast-like MG 63 cells response to the specimen (Lee et al., 2013; Peng et al., 2010; Yang et al., 2013; Zou et al., 2016).

Fig 6 shows SEM micrographs of the modified surface with non-porosities at 5A pulse current, 50μSec pulse on time and on different concentrations of SiC powder at high magnification (10000x). Nano-porosity with the presence of nano-cracks can be witnessed easily on the surface. Fig. 6 (a) shows the density and size of nano-porosities, with the concentration 5g/l. The size measured at 25000x magnification was 150-300nm.

While the concentration of powder increase up to 10g/l, the density, and size of the porosities reduced as shown in Fig. 6 (b) because SiC caused a decline in material transfer to the machined surface due to good flushing action. At 20g/l concentration, the improved density of porosities was observed all over the surface as shown in Fig 6 (c). At a greater level of magnification, the size of porosities was appeared to be 50-200nm. During machining action, eroded debris and powder particles deposit on workpiece surface which cause sudden quenching which causes the release in absorbed gasses generation nano-porosities. Lang et al., 2011 provide an improved biological environment for tissue growth and a powerful biological interface for the stability of the implant. The nano-surface morphology was remarkably affected by SiC powder concentration.

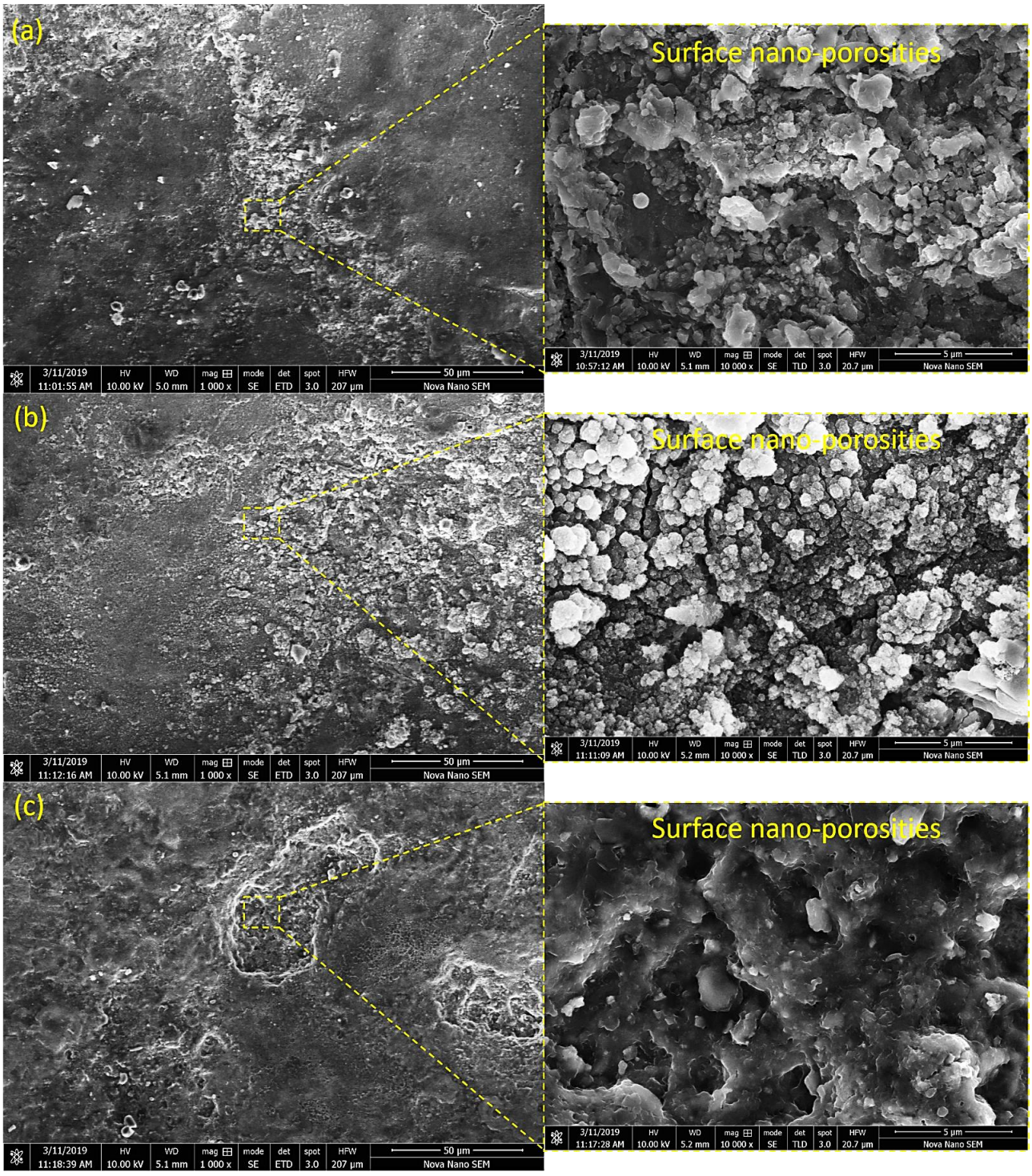

Figure 6. SEM micrographs showing nano-porosities of modified surface at IP 5A TON 50µSec with SiC powder mixed as concentration of (a) 5g/l (b) 10g/l (c) 20g/l at 10000x magnification

The improved nano-surface morphology increases hydrophilicity which favorably improve osseointegration (Lang et al., 2011). Overall microscale surface roughness and nanoscale surface topography improve osseointegration (Umar Farooq et al., 2020).

3.4 Surface Compositional and Quality Analysis:

Along with surface morphology, surface chemistry and composition also play a significant impact in biocompatibility. EDS analysis of the selected area in Fig 7 (a) and particle Fig 7 (b) confirms the particle migration from the powder to the workpiece surface.

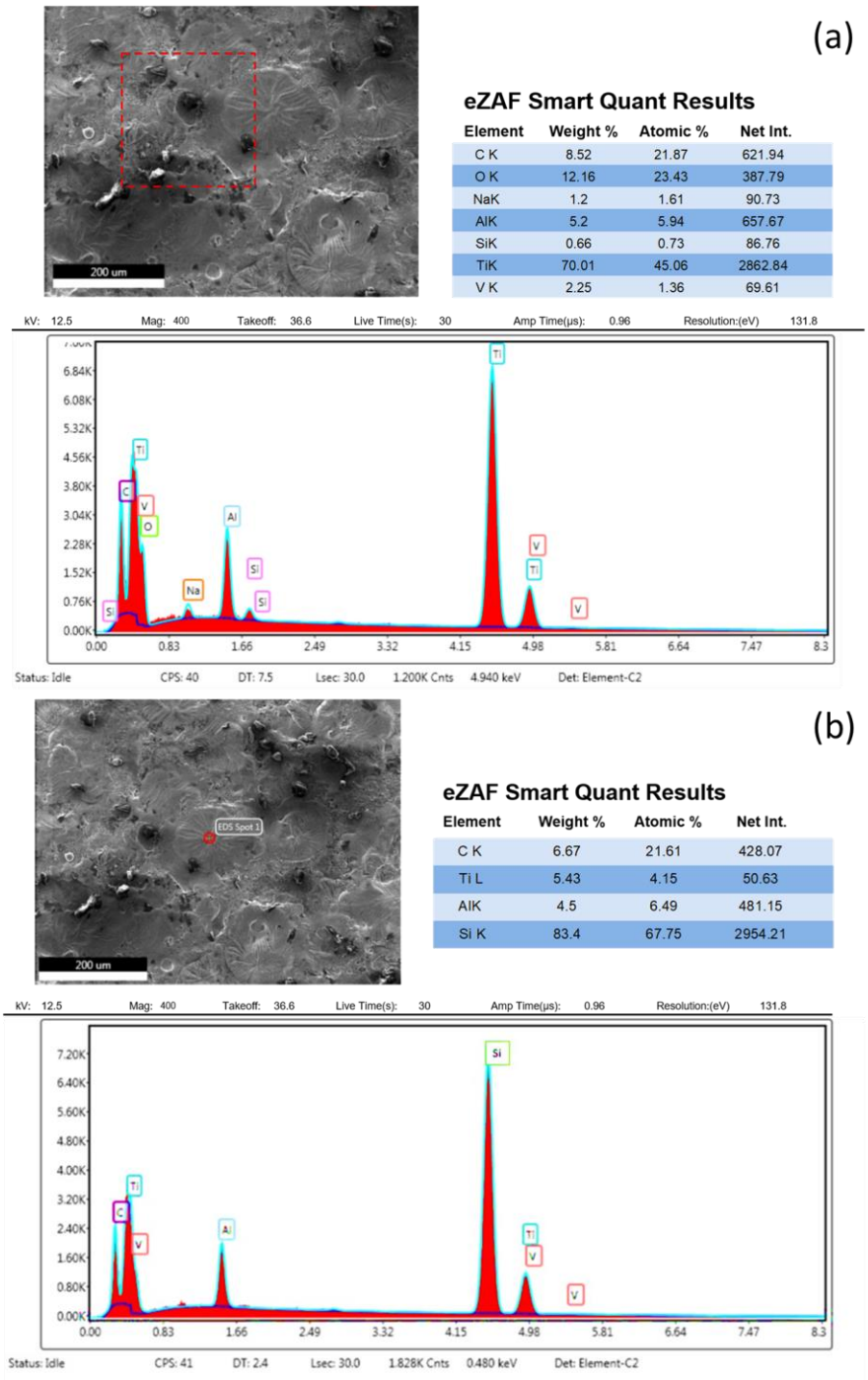

Figure 7. a) EDS analysis of Ti6Al4V ELI grade 23 modified surface (b) EDS analysis of selected particle, pulse current 5A, pulse on time 50µm, 20g/l powder concentration.

As it is confirmed from the previous discussion, PMEDM fabricated nano-porous structure which ultimately enhances osseointegration and corrosion resistance. The presence of TiO_2, SiO_2 and TiC (Prakash et al., 2015) are used as a surface coating to increase hardness, biocompatibility and corrosion resistance of implant. Initially, there would be no Si deposit on the machined surface (0g/l) but higher levels of O and C would be there due to electric discharge machining, decomposition of hydrocarbon oil at higher temperatures. The EDS analysis of the PMEDM surface confirmed the presence of oxygen and carbon which leads to the development of higher levels of carbides and oxides as shown in Fig 7 (a). Furthermore, the silicon deposit on the surface improves the biocompatibility. The deposit of Si leads to the formation of SiO_2 like phases which is confirmed by Fig 7 (b). The main effects plot for surface roughness shows that SR decreased from mean value ~6.5µm to ~3.7µm by increasing the concentration of powder from 0g/l to 5g/l. A further decrease can be witnessed by increasing concentration of powder in Fig 8 (a).

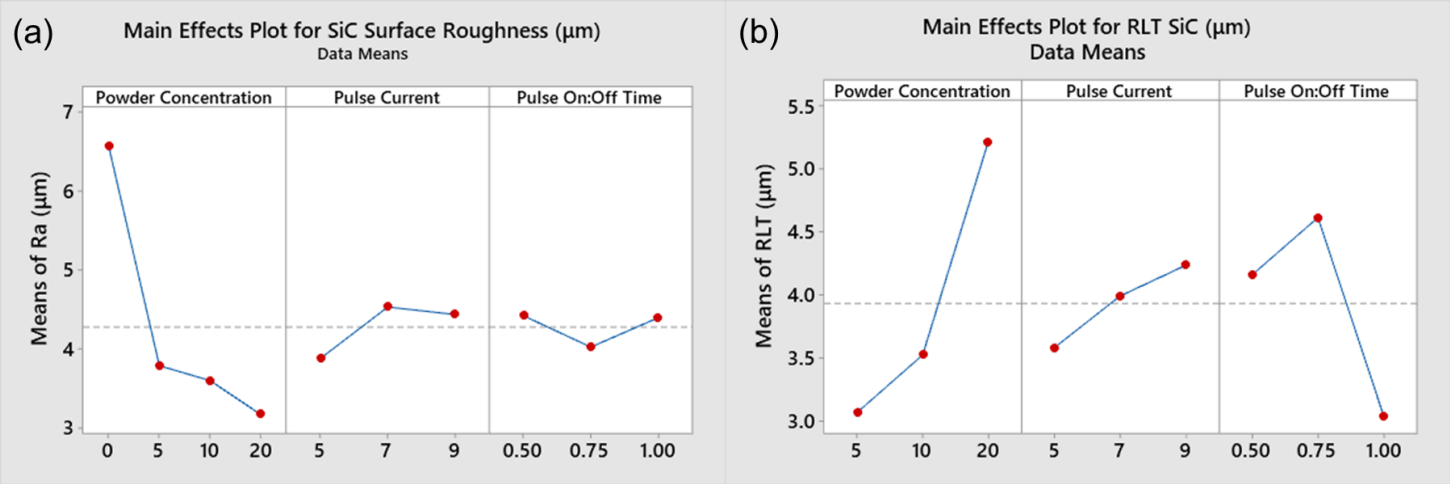

Figure 8. Trend plots of response characteristics (a) Surface roughness Ra (b) Recast layer thickness

The trend of SR is decreasing by increasing in SiC concentration of powder due to a balanced distribution of discharges and the enhanced interspace between tool and workpiece. SR decreases because SiC powder assisted in decreasing the heat intensity by dividing the discharges among powder particles ultimately decreasing the size of craters. Due to high discharge energy, by increasing pulse current, SR increased while a slight decrease in trend was witnessed on a higher level of the parameter. The reason behind the increase is that more metal was melted with more discharge energy creating ridges of molten metal and craters of intense sparks. The decrease is due to a short circuit produced between both electrodes, resulting in a slight decrease in SR. By

increasing pulse on time, due to cleaning cycles and proper distribution of discharges, SR is decreased but increased by a further increase in the parameter because of more energy transfer to the surface. Due to inadequate flushing and suspension of powder particles with molten debris increased recast layer from mean value ~12.5µm to ~20.5µm with an increase from 5g/l to 20g/l. High discharge energy was also found responsible for the high melt of metal and redeposition on the surface as shown in Fig 8 (b). The arcing between electrodes during the high frequency of discharges reduced the RLT with the help of flushing action. Microhardness of implant plays a vital role in wear resistance. A series of indentations for microhardness was done, which was two times of the indent diameter to nullify the effect of indent itself in the surroundings.

3.5 Surface Hardening:

The indentation was done one 20µm progressive distance from the previous indent. The maximum microhardness of 727HV was recorded at the highest concentration. While six indents in each sample were done to examine the behavior and phase changing of material until the base material characteristics obtained as shown in Fig 9.

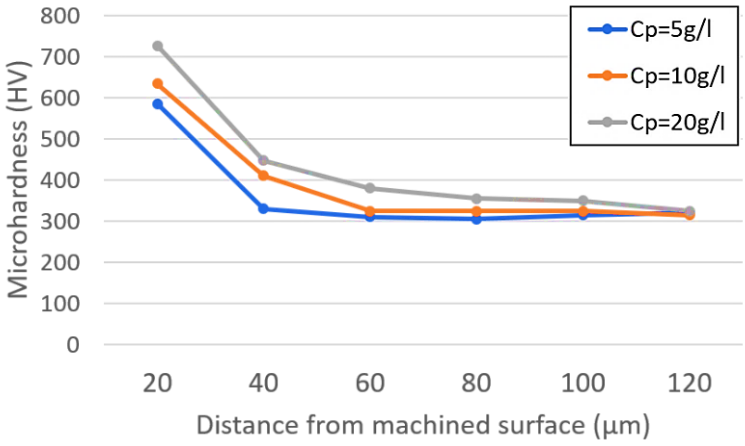

Figure 9. Micro hardness of machined samples at different powder concentrations and IP 5A, TON 50µSec.

The hardness is increased by increasing concentration of powder due to an increase in RLT and heat-affected zone. In biomedical applications, increased microhardness is beneficial in mechanical service (Mahbub et al., 2018).

The improved hardness is due to the growth of grain structure due to heating. While EDS analysis has confirmed the possibility of TiC, TiO2, and SiO2, etc. like carbides and oxides formation. These carbides and

oxides improve the hardness and other characteristics of the implant. The desirability function in Minitab 19 software was used to get optimized parameter settings for "minimum the better" RLT and surface roughness. The optimal settings obtained were 20g/l SiC powder concentration, 5A pulse current and 100µSec pulse on time while the other possibility is the same parameter settings with a 50µSec pulse on time with composite desirability 0.9363 and 0.8305, respectively. To sum up, biomedical based surface modification of Ti6Al4V ELI grade 23 has been carried out through SiC powder mixed EDM. Surface characteristics are investigated to decide the optimal process parameters to get the combination of desired surface characteristics, which is the novelty of the current study. The influence of different concentrations of powder was evaluated on microscale and nano-surface morphology.

4. Conclusions

Through rigorous discussion on all involved physical phenomenon and supported evidence, the following conclusions are extracted:

- The machining action without powder particles exhibited rough surface comprising cracks and surface pits. Whereas powder aided machining improved surface characteristics through polishing action and resulted in improved SR, RLT, MH. The concentration of powder (Cp) was examined the most impactful variable in SiC mixed EDM to control SR and RLT. The contribution of Cp to control the SR is 70.52%.
- With the addition in powder, the microhardness of the PM-EDMed surface almost doubled the hardness of bulk material and the surface texture was remarkably improved. The microhardness of the recast layer is more than the base material due to TiC, TiS_2 which improve microhardness from 320-727HV. The subsequent increase in I_P from 5-7A has correspondingly increased RLT from 12.5 µm to 13.8µm confirming the fact that RLT increases by increasing the concentration of a powder.
- Nano-porous bio-compatible surface (50-200nm) was generated in the workplace, providing control over the concentration of porosities on the modified surface. At greater density of SiC powder (20 g/l), the surface is anticipated to constitute of the oxide, Ti carbide, Si oxide, and Si carbide like phases. Silicon

deposit (0.66%) is confirmed on the surface proved by EDS analysis. Also, the breakdown of dielectric fluid is indicated by an increased level of carbon content.

- To capitulate, the finished machined surface obtained through SiC mixed EDM exhibit good surface morphology to minimize degree irregularities of the surface (i.e., surface roughness, micro-cracks, crater size, etc.) and improved porosity and chemistry against conventional EDM of Ti Alloy. The optimized combination of variables 20 g/l SiC powder, 5A pulse current and 100μs pulse of duration warrants comparably best surface attributes (SR and RLT).

In this work, the effect of SiC powder on Ti6Al4V ELI machining has been explicitly investigated, however, the variation in powder size is not studied which is the limitation of current research. In future, other potential powders can also be considered. Moreover, the work can be extended towards the investigation on the cell attachment and osseointegration to quantify the potentiality for specialized use.

References:

Abu Qudeiri, J.E., Mourad, A.-H.I., Ziout, A., Abidi, M.H., Elkaseer, A., 2018. Electric discharge machining of titanium and its alloys: review. Int J Adv Manuf Technol 96, 1319–1339. https://doi.org/10.1007/s00170-018-1574-0

Ahmed, M.H., Byrne, J.A., Keyes, T.E., Ahmed, W., Elhissi, A., Jackson, M.J., Ahmed, E., 2012. Characteristics and applications of titanium oxide as a biomaterial for medical implants, in: The Design and Manufacture of Medical Devices. Elsevier, pp. 1–57. https://doi.org/10.1533/9781908818188.1

Alavi, F., Jahan, M.P., 2017. Optimization of process parameters in micro-EDM of Ti-6Al-4V based on full factorial design. International Journal of Advanced Manufacturing Technology 92, 167–187. https://doi.org/10.1007/s00170-017-0103-x

AZOM Materials., 2020. Material Directory | Materials Engineering https://www.azom.com/ (accessed Jun 26, 2020).

Cai, K., Bossert, J., Jandt, K.D., 2006. Does the nanometre scale topography of titanium influence protein adsorption and cell proliferation? Colloids and Surfaces B: Biointerfaces 49, 136–144. https://doi.org/10.1016/j.colsurfb.2006.02.016

Chen, S.-L., Lin, M.-H., Chen, C.-C., Ou, K.-L., 2008. Effect of electro-discharging on formation of biocompatible layer on implant surface. Journal of Alloys and Compounds 456, 413–418. https://doi.org/10.1016/j.jallcom.2007.02.055

Çogun, C., Özerkan, B., Karaçay, T., 2006. An experimental investigation on the effect of powder mixed dielectric on machining performance in electric discharge machining. Proceedings of the Institution of Mechanical Engineers, Part B: Journal of Engineering Manufacture 220, 1035–1050. https://doi.org/10.1243/09544054JEM320

Dewangan, S., Gangopadhyay, S., Biswas, C.K., 2015. Study of surface integrity and dimensional accuracy in EDM using Fuzzy TOPSIS and sensitivity analysis. Measurement 63, 364–376. https://doi.org/10.1016/j.measurement.2014.11.025

Freese, H.L., Volas, M.G., Wood, J.R., Textor, M., 2001. Titanium and its alloy in biomedical engineering. Sci. and Tech., Elsevier Science Ltd 1–7.

Hadad, M., Bui, L.Q., Nguyen, C.T., 2018. Experimental investigation of the effects of tool initial surface roughness on the electrical discharge machining (EDM) performance. Int J Adv Manuf Technol 95, 2093–2104. https://doi.org/10.1007/s00170-017-1399-2

Hassanin, H., Al-Kinani, A.A., ElShaer, A., Polycarpou, E., El-Sayed, M.A., Essa, K., 2017. Stainless steel with tailored porosity using canister-free hot isostatic pressing for improved osseointegration implants. J. Mater. Chem. B 5, 9384–9394. https://doi.org/10.1039/C7TB02444D

Holmberg, J., Berglund, J., Wretland, A., Beno, T., 2019. Evaluation of surface integrity after high energy machining with EDM, laser beam machining and abrasive water jet machining of alloy 718. Int J Adv Manuf Technol 100, 1575–1591. https://doi.org/10.1007/s00170-018-2697-z

Jahan, M.P., Alavi, F., 2019. A Study on the Surface Composition and Migration of Materials and Their Effect on Surface Microhardness during Micro-EDM of Ti-6Al-4V. J. of Materi Eng and Perform 28, 3517–3530. https://doi.org/10.1007/s11665-019-04120-0

Kolli, M., Kumar, A., 2015. Effect of dielectric fluid with surfactant and graphite powder on Electrical Discharge Machining of titanium alloy using Taguchi method. Engineering Science and Technology, an International Journal 18, 524–535. https://doi.org/10.1016/j.jestch.2015.03.009

Kolli, M., Kumar, A., 2014. Effect of Boron Carbide Powder Mixed into Dielectric Fluid on Electrical Discharge Machining of Titanium Alloy. Procedia Materials Science 5, 1957–1965. https://doi.org/10.1016/j.mspro.2014.07.528

Kumar, P.M., Sivakumar, K., Jayakumar, N., 2018. Multiobjective optimization and analysis of copper–titanium diboride electrode in EDM of monel 400™ alloy. Materials and Manufacturing Processes 33, 1429–1437. https://doi.org/10.1080/10426914.2017.1415439

Kumar, S., Singh, R., Singh, T.P., Sethi, B.L., 2009. Surface modification by electrical discharge machining: A review. Journal of Materials Processing Technology 209, 3675–3687. https://doi.org/10.1016/j.jmatprotec.2008.09.032

Lang, N.P., Salvi, G.E., Huynh-Ba, G., Ivanovski, S., Donos, N., Bosshardt, D.D., 2011. Early osseointegration to hydrophilic and hydrophobic implant surfaces in humans: Early osseointegration on implant surfaces. Clinical Oral Implants Research 22, 349–356. https://doi.org/10.1111/j.1600-0501.2011.02172.x

Lee, W.F., Yang, T.S., Wu, Y.C., Peng, P.W., 2013. Nanoporous biocompatible layer on Ti-6Al-4V alloys enhanced osteoblast-like cell response. Journal of Experimental and Clinical Medicine(Taiwan) 5, 92–96. https://doi.org/10.1016/j.jecm.2013.04.002

Liang, J.F., Liao, Y.S., Kao, J.Y., Huang, C.H., Hsu, C.Y., 2018. Study of the EDM performance to produce a stable process and surface modification. International Journal of Advanced Manufacturing Technology 95, 1743–1750. https://doi.org/10.1007/s00170-017-1315-9

Mahbub, R., Jahan, M.P., Kirwin, R., Alavi, F., 2018. Micro-EDM induced surface modification of titanium alloy for biocompatibility. IJMMM 20, 274. https://doi.org/10.1504/IJMMM.2018.10014654

Malhotra, N., Rani, S., Singh, H., 2008. Improvements in performance of EDM-A review, in: IEEE SoutheastCon 2008. IEEE, pp. 599–603.

Miao, S., Lin, N., Cheng, K., Yang, D., Huang, X., Han, G., Weng, W., Ye, Z., 2011. Zn-Releasing FHA Coating and Its Enhanced Osseointegration Ability: Zn-Releasing FHA Coating and Enhanced Osseointegration Ability. Journal of the American Ceramic Society 94, 255–260. https://doi.org/10.1111/j.1551-2916.2010.04038.x

Mishra, R.R., Kumar, R., Sahoo, A.K., Panda, A., 2019. Machinability behaviour of biocompatible Ti-6Al-4V ELI titanium alloy under flood cooling environment. Materials Today: Proceedings.

Niinomi, M., 1998. Mechanical properties of biomedical titanium alloys. Materials Science and Engineering: A 243, 231–236. https://doi.org/10.1016/S0921-5093(97)00806-X

Öpöz, T.T., Yaşar, H., Ekmekci, N., Ekmekci, B., 2018. Particle migration and surface modification on Ti6Al4V in SiC powder mixed electrical discharge machining. Journal of Manufacturing Processes 31, 744–758. https://doi.org/10.1016/j.jmapro.2018.01.002

Park, J.-W., Kim, H.-K., Kim, Y.-J., An, C.-H., Hanawa, T., 2009. Enhanced osteoconductivity of micro-structured titanium implants (XiVE S CELLplus) by addition of surface calcium chemistry: a histomorphometric study in the rabbit femur. Clin Oral Implants Res 20, 684–690. https://doi.org/10.1111/j.1600-0501.2009.01714.x

Peng, P.-W., Ou, K.-L., Lin, H.-C., Pan, Y.-N., Wang, C.-H., 2010. Effect of electrical-discharging on formation of nanoporous biocompatible layer on titanium. Journal of Alloys and Compounds 492, 625–630. https://doi.org/10.1016/j.jallcom.2009.11.197

Prakash, C., Kansal, H.K., Pabla, B.S., Puri, S., 2017. Experimental investigations in powder mixed electric discharge machining of Ti–35Nb–7Ta–5Zrβ-titanium alloy. Materials and Manufacturing Processes 32, 274–285. https://doi.org/10.1080/10426914.2016.1198018

Prakash, C., Kansal, H.K., Pabla, B.S., Puri, S., 2015. Processing and Characterization of Novel Biomimetic Nanoporous Bioceramic Surface on β-Ti Implant by Powder Mixed Electric Discharge Machining. Journal of Materials Engineering and Performance 24, 3622–3633. https://doi.org/10.1007/s11665-015-1619-6

Sahu, S.K., Jadam, T., Datta, S., Nandi, G., 2018. Effect of using SiC powder-added dielectric media during electro-discharge machining of Inconel 718 superalloys. J Braz. Soc. Mech. Sci. Eng. 40, 330. https://doi.org/10.1007/s40430-018-1257-7

Saptaji, K., Gebremariam, M.A., Azhari, M.A.B.M., 2018. Machining of biocompatible materials: a review. International Journal of Advanced Manufacturing Technology 97, 2255–2292. https://doi.org/10.1007/s00170-018-1973-2

Shabgard, M., Khosrozadeh, B., 2017. Investigation of carbon nanotube added dielectric on the surface characteristics and machining performance of Ti–6Al–4V alloy in EDM process. Journal of Manufacturing Processes 25, 212–219. https://doi.org/10.1016/j.jmapro.2016.11.016

Simonis, P., Dufour, T., Tenenbaum, H., 2010. Long-term implant survival and success: a 10–16-year follow-up of non-submerged dental implants. Clinical oral implants research 21, 772–777.

Singh, A., Singh, R., 2015. Effect of Silicon Powder Mixed EDM on Surface Roughness of Al6063 Aluminium Alloy. International Journal for Innovative Research in Science & Technology 2, 182–186.

Singh, A.K., Mahajan, R., Tiwari, A., Kumar, D., Ghadai, R.K., 2018. Effect of Dielectric on Electrical Discharge Machining: A Review, in: IOP Conference Series: Materials Science and Engineering. IOP Publishing, p. 012184.

Sollazzo, V., Pezzetti, F., Scarano, A., Piattelli, A., Bignozzi, C., Massari, L., Brunelli, G., Carinci, F., 2008. Zirconium oxide coating improves implant osseointegration in vivo. Dental Materials 24, 357–361. https://doi.org/10.1016/j.dental.2007.06.003

Somashekhar, K.P., Ramachandran, N., Mathew, J., 2010. Optimization of material removal rate in micro-EDM using artificial neural network and genetic algorithms. Materials and Manufacturing Processes 25, 467–475. https://doi.org/10.1080/10426910903365760

Subramani, K., Mathew, R.T., Pachauri, P., 2018. Titanium surface modification techniques for dental implants—From microscale to nanoscale, in: Emerging Nanotechnologies in Dentistry. Elsevier, pp. 99–124. https://doi.org/10.1016/B978-0-12-812291-4.00006-6

Suresh, S., Jamil, M.A., Sulaiman, S., Shokor, M.R.M., 2016. Optimization of electrode material for EDM die-sinking of titanium alloy grade 5 - Ti6Al4V. International Journal on Advanced Science, Engineering and Information Technology 6, 534–539. https://doi.org/10.18517/ijaseit.6.4.902

Tiwary, A.P., Pradhan, B.B., Bhattacharyya, B., 2018. Investigation on the effect of dielectrics during micro-electro-discharge machining of Ti-6Al-4V. The International Journal of Advanced Manufacturing Technology 95, 861–874. https://doi.org/10.1007/s00170-017-1231-z

Umar Farooq, M., Pervez Mughal, M., Ahmed, N., Ahmad Mufti, N., Al-Ahmari, M.A., He, Y., 2020. On the Investigation of Surface Integrity of Ti6Al4V ELI Using Si-Mixed Electric Discharge Machining. Materials 13. https://doi.org/10.3390/ma13071549

Watanabe, Y., Sato, H., Miura-Fujiwara, E., 2015. Functionally Graded Metallic Biomaterials, in: Advances in Metallic Biomaterials. Springer, pp. 181–209.

Yang, T.-S., Huang, M.-S., Wang, M.-S., Lin, M.-H., Tsai, M.-Y., Wang Wang, P.-Y., 2013. Effect of Electrical Discharging on Formation of Nanoporous Biocompatible Layer on Ti-6Al-4V Alloys: Implant Dentistry 22, 374–379. https://doi.org/10.1097/ID.0b013e31829a170a

Ying, W.-S., Han, F.-Z., Wang, J.-H., 2017. Experimental investigation of fabricating diamond abrasive layers by EDM. The International Journal of Advanced Manufacturing Technology 93, 2111–2122.

Zeng, Y., Yang, Y., Chen, L., Yin, D., Zhang, H., Tashiro, Y., Inui, S., Kusumoto, T., Nishizaki, H., Sekino, T., Okazaki, J., Komasa, S., 2019. Optimized Surface Characteristics and Enhanced in Vivo Osseointegration of Alkali-Treated Titanium with Nanonetwork Structures. Int J Mol Sci 20. https://doi.org/10.3390/ijms20051127

Zou, R., Yu, Z., Li, W., Guo, M., Li, J., 2016. Influence of porous structure on the machining performance of micro EDM. Journal of Materials Processing Technology 232, 43–51. https://doi.org/10.1016/j.jmatprotec.2016.01.027

Table 1. Elemental composition of workpiece.

Element	Weight %
Al	5.860
V	3.940
Fe	0.134
O	0.100
C	0.017
N	0.008
H	0.00198
Ti	BAL
Sample size (n= 2)	

Table 2. Mechanical, electrical and thermal properties of Ti6Al4V ELI (AZOM Materials, 2020).

Property	Value	Unit
Hardness	320	Vicker D
Ultimate tensile strength	990	MPa
Density	4.43	g/cm^3
Modulus of elasticity	114	GPa
Yield strength	955	MPa
Electrical resistivity	178	μΩ-cm
Melting point	1660	^{o}C
Thermal conductivity	6.7	W/m-K

Table 3. Properties of electrode material (AZOM Materials, 2020).

Property	Value	Unit
Density	8.93	g/cm^3
Thermal conductivity	385	W/m-K
Melting point	1083	^{o}C
Linear expansion coefficient	16.4	10^{-6}/K
Electrical resistivity	1.7	μΩ-cm
Specific heat	385	J/kg K
Hardness	80-85	MPa

Table 4. Properties of SiC powder (Öpöz et al., 2018).

Property	Value	Unit
Shape of particle	Spherical	-
Nominal diameter	70-80	μm
Density	3.1	g/cm^3
Thermal conductivity	120	W/m-K
Electrical resistivity	0.01-1	μΩ-cm

Hardness	27.46	GPa
Color	Green	-

Table 5. List of variable control factors of EDM with their levels.

Variable	Units	Symbol	Levels		
			-1	0	+1
Powder Concentration	g/l	C_P	5	10	20
Pulse Current	A	I_P	5	7	9
Pulse Duration	µSec	$T_{ON/OFF}$	50/100	75/100	100/100
Sample size (n= 27)					

Table 6. List of fixed parameters.

Factor		Level
Voltage	Auxiliary (V)	(150-220)
	Spark (V)	5
Sensitivity	Arc	3
	Servo	4
Time	Spark (µsec)	5
	Flushing (µsec)	5
Dielectric	Oil	Kerosene

Table 7. Experimental parameters and their results without powder.

Exp.	Input Parameters			Results
	C_P (g/l)	I_P (A)	T_{ON} (µSec)	R_a (µm)
1	0	5	50	7.47
2	0	5	75	6.32
3	0	5	100	5.75
4	0	7	50	8.06
5	0	7	75	6.71
6	0	7	100	8.55
7	0	9	50	6.04
8	0	9	75	4.88
9	0	9	100	5.26

Table 8. Analysis of variance of surface roughness resulted from (0g/l powder concentration) EDM

Source	DF	Adj SS	Adj MS	F Value	P Value		PCR%
Pulse Current (A)	2	8.514	4.256	9.37	0.031*	Significant	67.68
Pulse on Time (µSec)	2	2.248	1.124	2.47	0.200	Non-Significant	17.87
Error	4	1.818	0.454				14.45
Total	8	12.579					100
Sample size (n= 9)							

*Significant at 95% confidence level

Table 9. Input parameters and results of PMEDM experimentation

Exp	Input parameters			Results	
	C_P (g/l)	I_P (A)	T_{ON} (µSec)	R_a (µm)	RLT (µm)
1	5	5	50	3.74	12.67
2	5	5	75	2.78	13.17
3	5	5	100	3.86	13.86
4	5	7	50	3.34	11.87
5	5	7	75	2.90	13.01
6	5	7	100	3.12	13.03
7	5	9	50	3.72	15.69
8	5	9	75	4.94	6.42
9	5	9	100	5.63	11.86
10	10	5	50	2.75	12.41
11	10	5	75	3.21	13.52
12	10	5	100	3.25	11.86
13	10	7	50	4.90	13.40
14	10	7	75	3.40	7.49
15	10	7	100	3.78	7.89
16	10	9	50	3.76	19.70
17	10	9	75	3.47	29.90
18	10	9	100	3.82	9.12
19	20	5	50	2.10	15.82
20	20	5	75	3.09	24.10
21	20	5	100	2.14	9.85
22	20	7	50	2.89	34.99
23	20	7	75	3.20	19.70
24	20	7	100	3.45	22.52
25	20	9	50	4.22	15.80
26	20	9	75	3.33	36.74
27	20	9	100	4.08	7.90

Table 10. ANOVA of surface roughness and recast layer thickness obtained by PMEDM

Surface roughness							
Source	DF	Adj SS	Adj MS	F Value	P Value		PCR %
A: C_p (g/l)	3	64.538	21.513	50.40	0.000*	Significant	70.55
B: Ip (A)	2	2.990	1.495	3.50	0.063	Non-Significant	3.27
C: T_{ON} (µSec)	2	1.185	0.592	1.39	0.287	-	1.30
A*B	6	14.530	2.421	5.67	0.005*	Significant	15.88
A*C	6	2.209	0.368	0.86	0.548	Non-Significant	2.42
B*C	4	0.900	0.225	0.53	0.718	-	0.98
Error	12	5.122	0.426				5.60
Total	35	91.476					100
Recast layer thickness							
Source	DF	Adj SS	Adj MS	F Value	P Value		PCR %
A: C_p (g/l)	2	362.84	181.42	4.29	0.05*	Significant	22.44
B: Ip (A)	2	38.14	19.07	0.45	0.652	Non-Significant	2.36
C: T_{ON} (µSec)	2	195.27	97.64	2.31	0.162	-	12.08
A*B	4	252.27	63.07	1.49	0.292	-	15.60
A*C	4	182.64	45.66	1.08	0.427	-	11.30
B*C	4	247.33	61.83	1.46	0.300	-	15.30
Error	8	338.34	42.29				20.92
Total	26	1616.84					100
Sample size (n= 27)							

*Significant at 95% confidence level